

July 6, 2019

Dear Dr Ciavatta,
Associate Editor, Biogeosciences

We are re-submitting our manuscript "*Rates and drivers of Red Sea plankton community metabolism*" to be considered for publication in Biogeosciences. In this revised version of the manuscript, we have addressed all your comments and made changes where suggested, specifically:

- 1) We have modified the abstract (see lines 9–11) and consistently reported throughout the text the calculated activation energy as positive (e.g., see lines 17, 284, 286, 359). We added a sentence to the methods section to clarify why we use E_a values and not $-E_a$ (obtained directly from the graphs) (please see lines 179-183).
- 2) We have specified the number of data included for the statistical analyses (e.g., lines 217–218, 226, 228) and consistently round the correlation coefficient values within the text and table 1.
- 3) Besides, we revised the manuscript for typos, and when needed, we improved specific sentences (e.g., line 42, 56–57).
- 4) We have included a new reference in line 84 (Lopez-Sandoval et al., 2019) as the study reported photosynthetic rates at different locations along the Red Sea.

Regarding the comment about statistical significance, we agree that a correlation does not mean causation or, as in our case, the lack of a significant relationship between metabolic rates and NO_x does not imply that nutrients do not play a role regulating planktonic metabolism. Throughout the manuscript, we aimed to emphasise that not only temperature but also nutrient availability must be a significant driver regulating the metabolic response of planktonic communities in the Red Sea, as GPP and CR rates peaked in the warmer and more nutrient-enriched area of the basin.

We do not think that the lack of relationship between metabolic rates and NO_x can be solely attributed to a reduced number of samples, which indeed was true ($n=56$ for NO_x , $n=77$ for metabolic rates). In our results, we showed that NO_x increased significantly from north to south in the surface layers and the bottom of the photic zone (Figure 3); however, this pattern was not evident when all data were taken in concert (data not shown). We also found that Chlorophyll-*a* concentration and metabolic rates were overall highest between these two layers, particularly in the southern Red Sea. Therefore, it seems conceivable to expect that there is an efficient consumption of nutrients occurring between these two layers, as NO_x remained mostly low and constant between the surface and the depth receiving 1% of surface PAR along the basin. The likely fast turnover rate of the nutrients pools (a common feature in oligotrophic environments) fuels planktonic metabolism whenever nutrients are available. This rapid turnover of nutrients seems to be particularly accentuated in the southern region, hence, explaining the positive relationship found between metabolic rates and latitude. Therefore, it is possible that because nutrient concentration remained relatively similar

within the area of higher productivity, we fail to see a correlation between metabolic rates and nutrient concentration.

We hope this explanation is satisfactory and that with the new changes you will find the revised version of the manuscript fulfils the quality and relevance necessary to be considered for publication in Biogeosciences.

Sincerely,

Daffne C. López-Sandoval
Red Sea Research Center
King Abdullah University of Science and Technology (KAUST)
Thuwal, Jeddah, 23955-6900, Kingdom of Saudi Arabia
Phone: (+966) 12 8082659

1 Rates and drivers of Red Sea plankton community metabolism

2 Daffne C. López-Sandoval¹, Katherine Rowe¹, Paloma Carillo-de-Albonoz¹, Carlos M. Duarte¹ and

3 Susana Agustí¹

4 ¹ Red Sea Research Center, King Abdullah University of Science and Technology (KAUST), Thuwal-Jeddah, 23955-6900,

5 Saudi Arabia

6 *Correspondence to:* Daffne C. López-Sandoval (daffne.lopezsandoval@kaust.edu.sa)

7 Abstract

8 Resolving the environmental drivers shaping planktonic communities is fundamental to understanding

9 their variability, in the present and the future, across the ocean. More specifically, addressing the

10 temperature-dependence response of planktonic communities is essential as temperature plays a key

11 role in regulating metabolic rates, thus potentially defining the ecosystem functioning. Here we

12 quantified plankton metabolic rates along the Red Sea, a uniquely oligotrophic and warm environment,

13 and analysed the drivers that regulate gross primary production (GPP), community respiration (CR) and

14 net community production (NCP). The study was conducted on six oceanographic surveys following a

15 north-south transect along the Saudi Arabian coast. Our findings revealed that GPP and CR rates

16 increased with increasing temperature ($R^2 = 0.41$ and 0.19 , respectively, $p < 0.001$ in both cases), with a

17 higher activation energy (E_a) for GPP (1.20 ± 0.17 eV) than for CR (0.73 ± 0.17 eV). The higher E_a for

18 GPP than for CR resulted in a positive relationship between NCP and temperature. This unusual

19 relationship is likely driven by 1) the relatively higher nutrient availability found towards the warmer

20 region (i.e., the south of the Red Sea), which favours GPP rates above the threshold that separates

21 autotrophic from heterotrophic communities ($1.7 \text{ mmol O}_2 \text{ m}^{-3} \text{ d}^{-1}$) in this region. 2) Due to the arid

22 nature, the basin lacks riverine and terrestrial inputs of organic carbon to subsidise a higher metabolic

23 response of heterotrophic communities, thus constraining CR rates. Our study suggests that GPP

Deleted: resolving

Deleted: to predict

Deleted: response of marine ecosystems to warming scenarios, as ocean warming leads to oligotrophication of the subtropical ocean

Deleted: the

Deleted: South

Deleted: demonstrates

31 increases steeply with increasing temperature in the warm ocean when relatively high nutrient inputs are
32 present.

33 1 Introduction

34 The balance between gross primary production and community respiration, which involves both
35 autotrophic and heterotrophic metabolic activity (Williams, 1993; Cullen, 2001; Ducklow and Doney,
36 2013), sets the metabolic status of an ecosystem by defining the carbon available to fuel pelagic food
37 webs and determining whether plankton communities act as a source or sink of CO₂ (Del Giorgio et al.,
38 1997; Williams, 1998). Whereas GPP typically satisfies the respiratory demands within the food web
39 across productive waters, the oligotrophic ocean often requires allochthonous inputs of organic carbon
40 to meet the metabolic requirements of heterotrophic organisms (Smith and Mackenzie, 1987). Due to
41 comparatively higher carbon consumption, relative to the production, planktonic communities in low
42 productivity systems are in close metabolic balance (i.e., $NCP = 0$, or $GPP = CR$) or experience a net
43 metabolic imbalance (i.e. $NCP < 0$, $GPP < CR$) (Smith and Hollibaugh, 1993; Duarte and Agustí, 1998;
44 Duarte et al., 2013).

45 In tropical and subtropical oligotrophic regions, the high temperatures may amplify the
46 metabolic imbalances in plankton communities, as CR tends to increase faster than GPP (Harris et al.,
47 2006; Regaudie-de-Gioux and Duarte, 2012) if the allochthonous sources of organic carbon are enough
48 to subsidise their carbon demand. These allochthonous inputs may be delivered from land through
49 riverine discharge, from the atmosphere through atmospheric deposition of dust and volatile organic

Deleted: productive

Deleted: the net community production (

52 carbon (Jurado et al., 2008), or are exported from productive coastal habitats (Duarte et al., 2013;
53 Barrón and Duarte, 2015).

54 The Red Sea is a semi-enclosed highly oligotrophic basin (Acker et al., 2008; Raitzos et al.,
55 2013). It is known as one of the warmest tropical seas, with maximum sea surface temperatures ranging
56 from 33.0 to 33.9 °C during summer (Chaidez et al., 2017; Osman et al., 2018), and up to 34–35 °C in
57 certain parts of the basin (Rasul and Stewart, 2015; Garcias-Bonet and Duarte, 2017; Almahasheer et
58 al., 2018). Due to the prevailing arid conditions, the Red Sea experiences large evaporation rates (nearly
59 2 cm yr⁻¹ of freshwater from the surface layers), while the lack of river runoff and low precipitation
60 rates make this system one of the saltiest seas on the planet (Sofianos, 2002; Sofianos and Johns, 2015;
61 Zarokanellos et al., 2017). Two wind patterns govern the region: in the northern part, the wind coming
62 from the northwest remains relatively constant throughout the year, while in the southern area, the
63 Indian Monsoon system regulates the wind dynamics (Sofianos, 2002; Sofianos and Johns, 2015).
64 During the winter monsoon, the wind changes direction, and this wind reversal along with the
65 thermohaline forces drives the overall circulation and favours the exchange of water with the Indian
66 Ocean (Sofianos, 2002; Zarokanellos et al., 2017).

67 Due to the almost negligible terrestrial inputs, the intrusion of nutrient-rich waters from the
68 Indian Ocean through the Bab-el-Mandeb Strait (Sofianos and Johns, 2007; Raitzos et al., 2015; Kürten
69 et al., 2016), together with aeolian dust and aerosol deposition (Chen et al., 2007; Engelbrecht et al.,
70 2017), represent the primary sources of nutrients into the basin. Thus, nutrient availability in the Red
71 Sea follows a latitudinal pattern that is opposite to the one of salinity, but parallel to the thermal

Deleted: the

Deleted: period

Deleted: between

Deleted: regions

76 gradient, with nutrient-rich and warmer waters towards the Southern Red Sea compared to the cooler
77 and more oligotrophic Northern Red Sea (Sofianos, 2002; Raitzos et al., 2015).

78 Studies based on ocean color data revealed that chlorophyll-a (Chl-a) concentrations decline
79 from the Southern Red Sea to the Northern Red Sea (Raitzos et al., 2013; Kheireddine et al., 2017;
80 Qurban et al., 2017) and depict a clear seasonality. During winter time, when the maximum exchange of
81 water with the Indian Ocean takes place, Chl-a concentration peaks, decreasing towards the summer
82 period when the water column is mostly stratified (Sofianos, 2002). Measurements of primary
83 production also revealed that phytoplankton photosynthetic rates follow the same south to north
84 gradient as Chl-a and nutrient concentration ([Qurban et al., 2017](#); [López-Sandoval et al., 2019](#)).

85 However, reports regarding the metabolic balance of the plankton communities are scarce, mostly focus
86 on the contribution of the autotrophic community via photosynthetic processes (Levanon-Spanier et al.,
87 1979; Qurban et al., 2014; Rahav et al., 2015), or are restricted to specific regions (Tilstra et al., 2018).

88 Based on available evidence, we hypothesise that the high gross primary production expected in
89 the Southern Red Sea may be counterbalanced by a higher respiratory demand in these warm waters,
90 and that NCP might decline towards the relatively unproductive waters of the Northern Red Sea. With
91 the expected decrease in GPP towards the northern region, planktonic metabolism might be driven
92 mainly by heterotrophic communities (Duarte and Agustí, 1998; Duarte et al., 2013). However, the
93 absence of significant allochthonous subsidies in the basin may hamper the metabolic response of the
94 heterotrophic plankton communities. Hence, it remains unclear what the metabolic balance of plankton
95 communities is and whether a south to north latitudinal gradient in NCP exists in the Red Sea.

96 Here we report the variability of plankton community metabolism (GPP, CR and NCP) along a
97 latitudinal gradient in the Red Sea, and examine if the temperature-dependence of planktonic metabolic
98 rates in this basin are consistent with those reported for the global ocean (López-Urrutia et al., 2006;
99 Regaudie-de-Gioux and Duarte, 2013; Garcia-Corral et al., 2017). We did so by conducting
100 measurements, as part of six surveys along the south-north latitudinal gradient in the Saudi Economic
101 Exclusive Zone in Red Sea waters. Specifically, we determined plankton metabolic rates between
102 winter 2016 and spring 2018, thus allowing us to 1) delineate the seasonal variability of the gross
103 primary production and community respiration along the Red Sea, 2) quantify changes in the metabolic
104 balance (net community production) and 3) test the hypothesized roles of productivity gradients and
105 temperature in driving NCP.

Deleted: conducted

Deleted: We

108 2. Material and Methods

109 2.1 Field Sampling

110 We conducted six oceanographic surveys: two during autumn (October and November 2016),
111 two during winter (February 2016 and January 2017), one in summer (August 2017), and one in spring
112 (March 2018) on board the R/V *Thuwal* and R/V *Al Azizi*. Sampling was conducted following a
113 latitudinal transect along the Red Sea within a region limited by coordinates 17.25 °N to 27.82 °N and
114 34.83 °E to 41.39 °E (Figure 1). At each station, vertical profiles of temperature and salinity were
115 obtained with a Sea-Bird SBE 911 plus CTD profiler (Sea-Bird Electronics, [Bellevue, WA, USA](#)),
116 equipped with additional sensors to measure the attenuation of photosynthetically active radiation
117 (PAR) (Biospherical/Licor PAR/Irradiance Sensor), *in vivo* fluorescence (WetLabs ECO FL
118 fluorometer), and dissolved oxygen concentration ([Sea-Bird SBE 43 Dissolved Oxygen Sensor](#)). Water
119 samples for chemical and biological measurements were collected between 7:00 and 9:00 am local time,
120 using a rosette sampler equipped with 12 Teflon Niskin bottles (12 L) that were provided with silicone
121 O-rings and seals.

122 2.2 Inorganic nutrients and chlorophyll-a concentration

123 Water samples for nutrient analyses were collected in 50 mL polyethene bottles and kept frozen
124 (-20 °C) until [further processing](#). Inorganic nutrient concentration was determined with a SEAL AA3
125 Segmented Flow Analyzer (SEAL Analytical Inc., WI, USA) using standard methods (Hansen and
126 Koroleff, 1999). The detection limits were 0.05 µM for nitrate, 0.01 µM for nitrite, 0.01 µM for

Deleted: Bellevue

Deleted: Seabird

Deleted: determination.

130 phosphate and 0.08 μM for silicate. For the chlorophyll-a analysis, 200 mL samples were taken at ten
131 discrete depths (between 5 and 200 m) and filtered through Whatman GF/F filters. The filters were kept
132 frozen (-20 °C) until further analysis. Pigments were extracted for 24 h using 90 % acetone and left
133 overnight in the dark at 4 °C. Chl-a concentration was estimated with the non-acidification technique
134 using a Trilogy Fluorometer equipped with CHL-NA module (Turner Designs, San Jose, USA),
135 previously calibrated with pure Chl-a.

136 **2.3 Net community metabolism, community respiration and gross primary production**

137 Plankton metabolic rates were determined *in vitro* by measuring the changes in dissolved
138 oxygen concentration after 24 h light-dark bottle (Winkler) incubations (Carpenter, 1965). This
139 methodology, commonly used to determine plankton metabolic rates (Williams et al., 1979; Duarte and
140 Agustí, 1998; Bender et al., 1999; Robinson and Williams, 1999; Ducklow et al., 2000; Serret et al.,
141 2001; Robinson et al., 2002; Serret et al., 2009; García-Martín et al., 2017), allows to account for the
142 diel cycle of oxygen and carbon fluxes derived from photosynthetic mechanisms (light-dependent
143 reactions) and also those linked to the acquisition of energy by both autotrophic and heterotrophic
144 microorganisms (light and dark-dependent reactions) (Robinson and Williams, 2005; Williams and del
145 Giorgio, 2005).

146 Water samples were collected at three different optical depths (ζ) through the water column.
147 One at the surface (100–80 % of incident PAR), another towards the bottom of the photic layer (8–1 %
148 of incident PAR), and one intermediate sample, at a depth of the chlorophyll maximum (Chl-*a* max). In
149 case the Chl-*a* max was sampled at the surface or bottom layers, the intermediate sample was taken

150 between 1.5–2.3 ζ (i.e., 22–10 % of incident PAR). Seawater was collected directly from the Niskin
151 bottles to fill a total of 21 (100 mL) Winkler bottles. The bottles were carefully filled using silicone
152 tubing and allowing the water to overflow during the filling, taking special care to avoid the formation
153 of air bubbles. Surface samples were collected in 100 mL quartz bottles. From each depth, seven of the
154 bottles were immediately fixed with Manganese ~~sulphate~~ (MnSO₄) and Potassium hydroxide/Potassium
155 iodide solution (KI/KOH) to determine the initial oxygen concentration while the other 14, seven light
156 and seven black bottles, were incubated on deck in surface water flow-through tanks. Due to the
157 difference in temperature between the surface and deep waters, particularly during the summer and
158 autumn surveys, we decided to include in our analyses only those samples collected above the
159 thermocline. Changes in temperature and PAR in the incubation tanks were recorded with HOBO
160 Pendant data loggers (Onset, Massachusetts, USA).

161 Before the incubation, the bottles were covered with neutral mesh to reduce the incident PAR
162 radiation according to the sampled depth. At the end of the incubation period, light and dark bottles
163 from each depth were fixed to determine final O₂ concentrations. Oxygen concentration was measured
164 by automated high-precision Winkler titration with a potentiometric end-point detection (Oudot et al.,
165 1988) using a Mettler Toledo T50 Titration Excellence auto-titrator attached to an Inmotion
166 autosampler. NCP was calculated as the difference in the oxygen concentration between the light bottles
167 after the 24 h incubation period ([O₂]_{L-24h}) and the oxygen concentration measured before the
168 incubation ([O₂]_{Tzero}) (i.e., NCP = ([O₂]_{L-24h} - [O₂]_{Tzero}). CR rates (mmol O₂ m⁻³ d⁻¹) were calculated as
169 the difference of the oxygen concentration after the 24 h incubation period in the dark bottles ([O₂]_D.

Deleted: sulfate

171 24h) and the initial oxygen concentration ($[O_2]_{Tzero}$) (i.e., $CR = [O_2]_{Tzero} - ([O_2]_{D-24h})$). GPP ($mmol\ O_2\ m^{-3}\ d^{-1}$) was calculated as the sum of NCP and CR.

173 Due to the consistent relationship existing between plankton metabolism and temperature across
174 diverse marine regions (Regaudie-de-Gioux and Duarte, 2012; García-Corral et al., 2014), we examined
175 how plankton metabolic rates covariate with temperature in the Red Sea, a system whose temperature
176 range is higher than previously encountered in marine planktonic metabolism research. We determined
177 the relationship between metabolic rates and temperature by fitting an ordinary least squares linear
178 regression equation to the relationship between the natural logarithm of the Chl-a specific metabolic
179 rates (B_0) and the inverse of the absolute temperature * k (i.e., $1/kT$), where k is the Boltzmann's
180 constant ($8.617734 \cdot 10^{-5}\ eV\ K^{-1}$) (Gillooly et al., 2001; Brown et al., 2004):

$$\ln B_0 = -Ea(1/kT) + C \quad (1)$$

182 In these so-called Arrhenius plots, the slope of this relationship represents the average activation energy
183 ($Ea = -slope$), characterising the extent of thermal-dependence of metabolic processes.

184 2.4 Statistical analyses

185 Statistical analyses and figures were done using the statistical and machine learning toolbox in
186 Matlab version R2018b (Mathworks Inc, Natick, MA, USA) and with the R statistical computing
187 package using RStudio 1.1419. Pearson correlation tests were used (corrplot function in R) to determine
188 the relationship between environmental variables (temperature, nitrate + nitrite (NOx), phosphate and
189 silicate concentration) and their latitudinal distribution, and to determine the relationship between
190 volumetric measurements of GPP, CR, NCP, and environmental variables (Temperature, NOx

Deleted: , which

Deleted:). In these Arrhenius plots, the slope represents the average activation energy (Ea), characterising the extent of thermal-dependence of metabolic processes.

Deleted: Analyses

196 concentration, Chl-*a*, and latitude). We used ordinary least squares (OLS) simple regression models
197 (fitlm function in Matlab) to describe the potential relationships between different planktonic metabolic
198 rates, between metabolic rates and environmental variables, and to predict the response of the Chl-*a*
199 normalised GPP (and CR) to temperature (Arrhenius plots described in section 2.3). To test if the
200 activation energies (obtained from the Arrhenius plots) were significantly different, we performed an
201 analysis of covariance (ANCOVA) by using the aocool in Matlab. The variability of planktonic
202 metabolic rates between cruises was statistically analysed using non-parametric Kruskal-Wallis tests.
203 Mean values and their standard error of the mean (SE) are reported throughout the text.

204 3. Results

205 3.1 Latitudinal variability of physico-chemical properties and Chl-*a* concentration

206 Hydrographic (temperature and salinity) and chemical variables (nutrient concentrations)
207 depicted a marked latitudinal gradient typical of the Red Sea. At the southern-most area, sea surface
208 temperature (SST) fluctuated between 28 °C (winter-spring) and 32 °C (summer), while at the far-
209 northern sampling site SST ranged between 23 °C (winter) and 27–28 °C (summer-autumn) (Figure 2).
210 Overall, all macronutrients observed a significant inverse correlation with latitude (Pearson correlation
211 coefficients $r \leq -0.4$, $p < 0.05$) (Figure 3). Nitrite+nitrate (NO_x) decreased from $6.1 \pm 0.9 \mu\text{M}$ in the
212 southern region to $2.9 \pm 0.3 \mu\text{M}$ towards the northern Red Sea, while on average, phosphate
213 concentration ranged from $0.5 \pm 0.01 \mu\text{M}$ in the south of the Red Sea to $0.1 \pm 0.01 \mu\text{M}$ towards the
214 northern stations (data not shown). Phytoplankton biomass (measured as Chl-*a* concentration) also

Deleted: °N

Deleted: <

217 decreased significantly towards the north of the Red Sea (Pearson's correlation, $r = -0.4$, $p < 0.001$, $n =$
218 77) (Table 1). We found the highest autotrophic biomass during the autumn and winter cruises. During
219 this period, surface Chl-a ranged from 0.6–0.8 mg m^{-3} in the southern region to 0.2–0.3 mg m^{-3} in the
220 north (Figure 2). In general, our results confirm that all variables correlated significantly with latitude,
221 highlighting the prevalence of the south-north gradient in temperature, salinity, nutrient availability and
222 chlorophyll-a concentration across the Red Sea.

223 3.2 Variability of plankton metabolism measured along the Red Sea

224 Analogous to the environmental variability, planktonic metabolism followed the same
225 significant north-south decreasing pattern with latitude (Figure 4). The inverse correlation of GPP rates
226 with latitude was highly significant (Pearson correlation coefficient $r = -0.6$, $p < 0.001$, $n = 77$) (Table
227 1), as found for autotrophic biomass, thus, explaining the strong correlation observed between GPP and
228 Chl-a concentration (Pearson correlation coefficient $r = 0.7$, $n = 77$) (Table 1). GPP rates decreased on
229 average by 79%, from $4.1 \pm 0.5 \text{ mmol O}_2 \text{ m}^{-3} \text{ d}^{-1}$ ($\approx 49.2 \text{ mgC m}^{-3} \text{ d}^{-1}$; assuming a photosynthetic
230 quotient, $\text{PQ} = 1$) at the southernmost station of the Red Sea to 0.9 ± 0.1 ($\approx 10 \text{ mgC m}^{-3} \text{ d}^{-1}$; $\text{PQ} = 1$) at
231 the northern site, while CR decreased on average by 73 %, from $3 \pm 0.4 \text{ mmol O}_2 \text{ m}^{-3} \text{ d}^{-1}$ ($\approx 36 \text{ mgC m}^{-3}$
232 d^{-1} ; assuming a respiratory quotient, $\text{RQ} = 1$) in the south to 0.8 ± 0.1 in the north ($\approx 9.6 \text{ mgC m}^{-3} \text{ d}^{-1}$;
233 $\text{RQ} = 1$) (Figure 4). We did not find any significant correlation between NO_x availability and GPP
234 (Pearson correlation coefficient, $p > 0.05$, $n = 56$), CR (Pearson correlation coefficient, $r = 0.2$, $p >$
235 0.05) nor NCP rates (Pearson correlation coefficient, $r = -0.2$, $p > 0.05$, $n = 56$) (Table 1); however, all
236 metabolic rates were positively correlated with temperature (Table 1).

Deleted: 41

Deleted: 60

Deleted: 69

Deleted: $r = 0.01$,

Deleted: 19

Deleted: 19

243 The highest GPP and CR rates measured along the Red Sea came from data collected during the
 244 autumn and winter cruises, when GPP and CR rates reached values above 6 and 4 mmol O₂ m⁻³ d⁻¹,
 245 respectively (Figure 5), and when the mean values were the highest (GPP_{autumn-winter} = 2.9 ± 0.3 – 2.3 ±
 246 0.3 mmol O₂ m⁻³ d⁻¹; CR_{autumn-winter} = 2.5 ± 0.3 – 2 ± 0.2) (Figure 5). However, despite the overall
 247 variability between autumn-winter and spring-summer, when all data are taken in concert, planktonic
 248 GPP and CR rates were not significantly different between seasons (Kruskal-Wallis H test, $\chi^2 = 6.83$, p
 249 = 0.08; $\chi^2 = 4.14$, p = 0.25, respectively). Furthermore, the balance between planktonic autotrophic
 250 production (GPP) and respiratory losses (due to the heterotrophic and autotrophic metabolism, CR) (i.e.,
 251 NCP rates) revealed that NCP rates also decreased towards the northern region (by 94%). From 1.1 ±
 252 0.3 mmol O₂ m⁻³ d⁻¹ at the southern stations to 0.1 ± 0.1 mmol O₂ m⁻³ d⁻¹ above 26 °N (Figure 4). The
 253 average NCP measured during our cruises was 0.3 ± 0.1 mmol O₂ m⁻³ d⁻¹ (Figure 5), which indicates an
 254 overall prevalence of autotrophic communities (Figure 5). However, a closer look at our data revealed
 255 the mean NCP rate in spring was -0.3 ± 0.2 mmol O₂ m⁻³ d⁻¹ (Figure 5), while during summer, NCP
 256 rates in the northern region ranged from -0.6 to -0.1 mmol O₂ m⁻³ d⁻¹, which evidenced that planktonic
 257 metabolism was governed by heterotrophic communities during both spring and summer in the northern
 258 region.

259 When we evaluated the relationship of GPP with CR and NCP, the analysis showed that both
 260 CR and NCP increased significantly with GPP (R² = 0.62 and 0.49, respectively; p < 0.001) (Figure 6).
 261 From the functional relationships between GPP with CR and NCP, we calculated the threshold of GPP
 262 for metabolic equilibrium for the region. By solving for GPP=CR and for NCP = 0 (from the
 263 relationship describing NCP as a function of GPP), and by using the slope and intercept shown in

Deleted: the

Deleted:),

Deleted: from

Deleted: to

Deleted: that during spring,

Deleted: 1

Deleted: 4

Deleted: the

Deleted: 4

Deleted: 09

Deleted: the

Deleted: also during the

Deleted: at

277 figures 6A and 6B, we determined that the GPP threshold that separates autotrophic from heterotrophic
278 planktonic communities in the Red Sea is $1.7 \text{ mmol O}_2 \text{ m}^{-3} \text{ d}^{-1}$ (range $1.2\text{--}1.9 \text{ mmol O}_2 \text{ m}^{-3} \text{ d}^{-1}$).

279 3.3 Metabolic rates and temperature

280 Due to the pervasive influence of temperature in regulating metabolic rates, we further explored
281 the temperature-dependence of GPP and CR by analysing the relationship between chlorophyll-a
282 specific metabolic rates and temperature. Our analysis revealed that both GPP and CR tended to
283 increase with temperature albeit with different activation energies (i.e., E_a was significantly higher for
284 GPP ($1.20 \pm 0.17 \text{ eV}$) than for CR rates ($0.73 \pm 0.17 \text{ eV}$), ANCOVA, $F = 3.96$, $p = 0.04$) (Figure 7). We
285 also tested whether the temperature-dependence response was consistent between cruises (Figure 8).

286 Our results indicated a relatively higher activation energy for GPP during the summer cruise ($2.31 \pm$
287 0.75 eV) and for CR in spring ($2.60 \pm 0.85 \text{ eV}$). However, the observed differences in the activation
288 energies for GPP were not significantly different between seasons (ANCOVA, $F = 0.38$, $p = 0.8$).

289

- Deleted: (-
- Deleted: 2
- Deleted: (-
- Deleted: 2
- Deleted: 4
- Deleted: (-
- Deleted: 8
- Deleted: for CR (-
- Deleted: 9

299 4. Discussion

300 4.1 Variability of plankton community metabolic rates along the Red Sea

301 Our results demonstrate that planktonic metabolic rates are markedly different between the
302 southern and northern regimes of the Red Sea, with a northward increase in the overall mean GPP and
303 CR by a factor of 5 and 4, respectively (i.e., an absolute increase in GPP rates of $3.2 \text{ mmol O}_2 \text{ m}^{-3} \text{ d}^{-1} \approx$
304 $38.4 \text{ mgC m}^{-3} \text{ d}^{-1}$, while absolute CR rates increased by $2.2 \text{ mmol O}_2 \text{ m}^{-3} \text{ d}^{-1} \approx 26.4 \text{ mgC m}^{-3} \text{ d}^{-1}$).
305 Although, *sensu stricto*, the overall balance between autotrophic metabolism and planktonic community
306 respiration (i.e. NCP) indicated a prevalence of autotrophic communities during our samplings along the
307 Red Sea, heterotrophic communities prevailed during the spring, and in the northern stations during the
308 summer, which highlights the shift in the trophic conditions in the basin. Consistent with these findings,
309 our data revealed that the GPP threshold that separated autotrophic from heterotrophic communities in
310 the Red Sea ($1.7 \text{ mmol O}_2 \text{ m}^{-3} \text{ d}^{-1}$) is similar to that reported across oceanic communities elsewhere
311 (Duarte and Agustí, 1998; Duarte and Regaudie-de-Gioux, 2009), agreeing with the oligotrophic
312 characteristics that govern the basin at certain periods or locations. The latitudinal differences depicted
313 in our results mirror the increasing north-south pattern in Chl-*a* concentration and photosynthetic carbon
314 fixation rates previously reported for the Red Sea (Acker et al., 2008; Raitso et al., 2013; Qurban et al.,
315 2014; Kheireddine et al., 2017), and which are supported by the presence of different planktonic
316 communities (Al-aidaroos et al., 2016; Pearman et al., 2016; Robitzch et al., 2016; Kheireddine et al.,
317 2017; Kottuparambil and Agusti, 2018).

318

Deleted: an

Deleted: from the southern to the northern regions

Deleted: and an

Deleted: increase in

Deleted: of

Deleted: the basin

325 The lower productivity of the northern section of the Red Sea explains the dominance of
326 heterotrophic communities therein. Still, sustaining heterotrophy in oligotrophic regions requires an
327 allochthonous source of organic matter (Duarte et al. 2011, 2013). The arid nature of the northern Red
328 Sea, with the watershed consisting mostly of deserts, leads to the absence of rivers and significant
329 organic carbon inputs to the sea. Dust inputs are important, however, and whereas they have shown no
330 effect on primary production (Torfstein and Kienast, 2018), they are a source of organic carbon (Jurado
331 et al. 2009) that can partially supply the organic matter required to sustain heterotrophic communities.

Deleted: .

332 Moreover, the Red Sea supports highly productive coral reefs, mangrove forests, seagrass meadows and
333 algal communities in its extensive shallow coastal areas (Rasul et al., 2015; Almahasheer et al., 2016),
334 which may export significant organic carbon to the pelagic compartment, thereby helping to sustain
335 heterotrophic plankton communities in the northern Red Sea.

Deleted: reef

Deleted: the

336 4.2 Temperature and metabolic balance in the Red Sea

337 Temperature is a master variable that regulates many components of ocean dynamics, such as
338 vertical stratification, and most aspects of organismal biology, from setting boundaries in the distribution
339 of organisms (Clarke, 1996) to controlling biochemical reactions that constrain the energy for metabolic
340 processes (Gillooly et al., 2001). Hence, temperature is likely a significant driver of metabolic processes
341 in the Red Sea, one of the warmest tropical marine ecosystems (Raitsois et al., 2011; Chaidez et al.,
342 2017). Indeed, our results showed a positive response of planktonic metabolism to temperature.
343 Moreover, the functional relationships between metabolic rates with temperature suggested that both
344 GPP and CR were positively enhanced with increasing temperature; but at a different pace.

Deleted: ,

349 The metabolic theory of ecology (MTE) relates the metabolic rate of an organism with its mass
350 and temperature. This theory hypothesizes that individual metabolic rates relate to temperature with a
351 relatively constant activation energy ($E_a \sim 0.63$ eV) for a wide range of taxa, from unicellular organisms
352 to plants and animals (Gillooly et al., 2001; Brown et al., 2004). For aerobic respiration, E_a values vary
353 between 0.41 and 0.74 eV at temperatures between 0–40 °C (Gillooly et al., 2005), while for
354 photosynthetic processes, the predicted E_a is lower, ~ 0.32 eV (Allen et al., 2005). From a thorough
355 compilation of data obtained for a wide range of marine systems (from polar to subtropical and tropical
356 oceanic regions), Regaudie-de-Gioux and Duarte (2012) found that overall, the activation energies for
357 photosynthetic production (GPP) varied between 0.29–0.32 eV, and for respiratory processes (CR)
358 between 0.65 and 0.66 eV.

359 The E_a for GPP (1.20 ± 0.17 eV) obtained for the Red Sea was higher than the overall value
360 predicted by the MTE, while the E_a values for CR were below those for GPP (0.72 ± 0.17 eV) unlike
361 observed elsewhere in open oceanic waters (Regaudie-de-Gioux and Duarte 2011, Garcia-Corral et al.
362 2017). Furthermore, these E_a values imply that GPP rates increased faster (5.1-fold) than CR rates (2.7-
363 fold), in the Red Sea's thermal range (22–32.5 °C). These findings differ with the expected double
364 increase of heterotrophic respiration (regarding photosynthetic processes) with temperature (Harris et
365 al., 2006), but are closer to results obtained by Garcia-Corral et al. (2017), who recently reported E_a for
366 GPP of 0.86 , 1.48 and 1.07 eV for the Atlantic, Indian, and Pacific oceans, respectively, while E_a for
367 CR found in the Atlantic, Indian and the Pacific oceans were 0.77, 0.57 and 0.82 eV, respectively.

368 The apparent contradiction between our findings and the general patterns predicted by the MTE
369 is, however, not surprising. In their model, Allen et al. (2005) predict the activation energy of

Deleted: (-

Deleted: activation energies

Deleted: -

Deleted: -

Deleted: -

Deleted: -

Deleted: -

Deleted: -

378 photosynthesis per chloroplast (for temperatures between 0–30 °C) using the temperature dependence
379 parameters obtained by Bernacchi et al. (2001) for RuBisCO carboxylation rates in one species (tobacco
380 leaves). Although the temperature range selected by Allen et al. (2005) comprises the optimum
381 temperatures of growth rates for a wide range of functional groups of marine primary producers (Chen,
382 2015; Thomas et al., 2016), the temperature observed in the Red Sea exceeded this range. Due to the
383 fast generation times of microbes (Collins, 2010), we can expect that photosynthetic planktonic
384 communities are acclimated or even locally adapted to the thermal conditions they experience. So by
385 favouring certain photosynthetic or thermal traits, they can enhance their metabolism and growth to the
386 ambient temperature, up to their thermal optimum (Galmes et al., 2015; Thomas et al., 2016).
387 Therefore, it is likely that the acclimation or local adaptation (in the long term) of photosynthetic traits
388 in Red Sea plankton optimises the metabolic response at the high temperatures reached, resulting in a
389 steeper response to temperature than predicted by the MTE. Moreover, as the trait responses to
390 temperature vary among phylogenetic groups (Galmes et al., 2015; Galmés et al., 2016; Thomas et al.,
391 2016), we anticipated a certain degree of discrepancy if we characterise the photosynthetic response
392 (GPP) of planktonic communities by considering only one trait (i.e., RuBisCO carboxylation) of one
393 species.

394 However, we must bear in mind that the metabolic response of individuals is not only
395 temperature-dependent, and that resource supply also plays an essential role (Brown et al., 2004; Allen
396 and Gillooly, 2009). Our results evidenced that the increased response of planktonic metabolism
397 towards warmer temperatures was mostly confined to the southern half of the Red Sea, which receives
398 the direct inflow of the enriched Intermediate Water coming from the Gulf of Aden during the winter

Deleted: temperatures they experience

Deleted: -

Deleted: forming an ecosystem,

Deleted: a region that

403 monsoon (Raitos et al., 2015; Wafar et al., 2016). Recent findings have demonstrated that mass-
404 specific carbon fixation rates of phytoplankton communities can be enhanced with increasing
405 temperature when nutrients are not limiting their growth (Marañón et al., 2014; Marañón et al., 2018).
406 Therefore, it is likely that the intertwined effect of both the warmer temperatures and the higher nutrient
407 availability towards the south of the Red Sea are key drivers regulating the metabolic response of
408 planktonic communities. Thus, unlike the global ocean, where nutrient concentration is inversely
409 correlated with temperature (e.g., Agawin et al. 2000), in the Red Sea nutrient concentration and
410 temperature are positively correlated. This anomaly may explain the steep increase in E_a for GPP, as
411 primary producers in the warmer region are being supported by the inflow of nutrient-enriched waters
412 from the Indian Ocean.

413 The elevated E_a for GPP compared to CR in Red Sea plankton is also an anomaly, likely
414 associated with the lack of allochthonous nutrient supply due to the absence of rivers and vegetation in
415 the arid watershed of the Red Sea. The warm oligotrophic ocean is characterised by plankton
416 communities that are in metabolic balance or net metabolically imbalanced (Duarte and Agusti 2008,
417 Duarte et al. 2013). In contrast, the warm Southern Red Sea tends to support autotrophic metabolism,
418 sustained by the input of nutrient-enriched waters while low allochthonous carbon inputs may constrain
419 CR. As a result, NCP tends to increase, rather than decrease with increasing temperature (Regaudie-de-
420 Gioux and Duarte 2011, Garcia-Corral et al. 2017). These patterns in plankton metabolism in the
421 oligotrophic and warm Red Sea deviate from those characterising the subtropical and tropical gyres of
422 the open ocean, but it provides an opportunity to explore the mechanistic basis for patterns in plankton

Deleted: larger

Deleted: the

Deleted: metabolic

Deleted: the global

427 metabolism with temperature, which would otherwise remain obscured by the underlying prevalent
428 negative relationship with nutrient concentrations.

429 5. Conclusions

430 Our results show that plankton metabolism in the Red Sea presents a remarkably different
431 pattern compared to other warm and oligotrophic marine systems (e.g., the subtropical and tropical
432 gyres). In this region, autotrophic plankton communities prevailed and are supported by relatively high
433 GPP rates; above the threshold separating heterotrophic low-productivity communities from autotrophic
434 ones. Metabolically-balanced or net heterotrophic plankton communities dominated in the Northern Red
435 Sea, whereas autotrophic communities, were predominant in the south supported by nutrient inputs from
436 the Gulf of Aden. Elevated temperatures contributed to the enhanced metabolic activity of planktonic
437 organisms due to the increase in kinetic energy (favouring enzymatic reactions) with temperature.
438 Plankton communities in the Red Sea, however, displayed activation energies for GPP that were higher
439 than those for CR, resulting in a positive relationship between NCP and temperature. Those findings
440 represent anomalies in the relationship between metabolic rates and temperature compared to the warm,
441 oligotrophic open ocean. These anomalies are likely related to the higher nutrient supply from nutrient-
442 rich Indian Ocean waters in the warm Southern Red Sea, suggesting that GPP can respond strongly to
443 the temperature in the warm ocean when supported by high nutrient inputs, relative to those in the
444 subtropical gyres.

Deleted: supported by nutrient inputs from the Gulf of Aden,

Deleted: an

447 **Author Contributions**

448 DCL-S, CMD, and SA designed the study; KR and PCdA obtained the data and provided technical
449 support; DCL-S analysed the data; DCL-S wrote the article with a substantial contribution of CMD, and
450 SA; all authors discussed the results and commented on the manuscript.
451

452 **Acknowledgements**

453 The research reported in this publication was supported by funding from King Abdullah University of
454 Science and Technology (KAUST), under award number BAS/1/1071-01-10 assigned to CMD,
455 BAS/1/1072-01-01 assigned to SA, and CCF/1/1973-21-01 assigned to the Red Sea Research Center.

456 References

- 457 Acker, J., Leptoukh, G., Shen, S., Zhu, T., and Kempler, S.: Remotely-sensed chlorophyll a observations of the northern Red Sea indicate
458 seasonal variability and influence of coastal reefs, *Journal of Marine Systems*, 69, 191-204, 10.1016/j.jmarsys.2005.12.006, 2008.
- 459 Agawin, N. S., Duarte, C. M., and Agustí, S.: Nutrient and temperature control of the contribution of picoplankton to phytoplankton biomass
460 and production, *Limnology and Oceanography*, 45, 591-600, 2000.
- 461 Al-aidaroos, A. M., Karati, K. K., El-sherbiny, M. M., Devassy, R. P., and Kürten, B.: Latitudinal environmental gradients and diel variability
462 influence abundance and community structure of Chaetognatha in Red Sea coral reefs, *Systematics and Biodiversity*, 15, 35-48,
463 10.1080/14772000.2016.1211200, 2016.
- 464 Almahasheer, H., Abdulaziz, A., and Duarte, C. M.: Decadal stability of Red Sea mangroves, *Estuarine Coastal and Shelf Science*, 169, 164-
465 172, 2016.
- 466 Almahasheer, H., Duarte, C. M., and Irigoien, X.: Leaf Nutrient Resorption and Export Fluxes of *Avicennia marina* in the Central Red Sea
467 Area, *Frontiers in Marine Science*, 5, 10.3389/fmars.2018.00204, 2018.
- 468 Allen, A., Gillooly, J., and Brown, J.: Linking the global carbon cycle to individual metabolism, *Functional Ecology*, 19, 202-213, 2005.
- 469 Allen, A. P., and Gillooly, J. F.: Towards an integration of ecological stoichiometry and the metabolic theory of ecology to better understand
470 nutrient cycling, *Ecol Lett*, 12, 369-384, 10.1111/j.1461-0248.2009.01302.x, 2009.
- 471 Barrón, C., and Duarte, C. M.: Dissolved organic carbon pools and export from the coastal ocean, *Global Biogeochemical Cycles*, 29, 1725-
472 1738, 2015.
- 473 Bender, M., Orchardo, J., Dickson, M.-L., Barber, R., and Lindley, S.: In vitro O₂ fluxes compared with 14 C production and other rate
474 terms during the JGOFS Equatorial Pacific experiment, *Deep Sea Research Part I: Oceanographic Research Papers*, 46, 637-654, 1999.
- 475 Bernacchi, C., Singas, E., Pimentel, C., Portis Jr, A., and Long, S.: Improved temperature response functions for models of Rubisco-limited
476 photosynthesis, *Plant, Cell & Environment*, 24, 253-259, 2001.
- 477 Brown, J. H., Gillooly, J. F., Allen, A. P., Savage, V. M., and West, G. B.: Toward a metabolic theory of ecology, *Ecology*, 85, 1771-1789,
478 2004.
- 479 Carpenter, J. H.: The accuracy of the Winkler method for dissolved oxygen analysis, *Limnology and Oceanography*, 10, 135-140, 1965.
- 480 Clarke, A.: The influence of climate change on the distribution and evolution of organisms, *Animals and Temperature. Phenotypic and*
481 *Evolutionary Adaptation*, 377-407, 1996.
- 482 Collins, S.: Many Possible Worlds: Expanding the Ecological Scenarios in Experimental Evolution, *Evolutionary Biology*, 38, 3-14,
483 10.1007/s11692-010-9106-3, 2010.
- 484 Cullen, J.: Primary production methods, *Marine Ecology Progress Series*, 52, 88, 2001.
- 485 Chaidez, V., Dreano, D., Agustí, S., Duarte, C. M., and Hoteit, I.: Decadal trends in Red Sea maximum surface temperature, *Scientific*
486 *Reports*, 7, 8144, 10.1038/s41598-017-08146-z, 2017.
- 487 Chen, B.: Patterns of thermal limits of phytoplankton, *Journal of Plankton Research*, 37, 285-292, 10.1093/plankt/fbv009, 2015.
- 488 Chen, Y., Mills, S., Street, J., Golan, D., Post, A., Jacobson, M., and Paytan, A.: Estimates of atmospheric dry deposition and associated
489 input of nutrients to Gulf of Aqaba seawater, *Journal of Geophysical Research: Atmospheres*, 112, 2007.
- 490 Del Giorgio, P. A., Cole, J. J., and Cimleris, A.: Respiration rates in bacteria exceed phytoplankton production in unproductive aquatic
491 systems, *Nature*, 385, 148, 1997.
- 492 Duarte, C. M., and Agustí, S.: The CO₂ balance of unproductive aquatic ecosystems, *Science*, 281, 234-236, 1998.
- 493 Duarte, C. M., and Regaudie-de-Gioux, A.: Thresholds of gross primary production for the metabolic balance of marine planktonic
494 communities, *Limnology and Oceanography*, 54, 1015-1022, 2009.
- 495 Duarte, C. M., Regaudie-de-Gioux, A., Arrieta, J. M., Delgado-Huertás, A., and Agustí, S.: The Oligotrophic Ocean Is Heterotrophic, *Annual*
496 *Review of Marine Science*, 5, 551-569, 10.1146/annurev-marine-121211-172337, 2013.
- 497 Ducklow, H. W., Dickson, M.-L., Kirchman, D. L., Steward, G., Orchardo, J., Marra, J., and Azam, F.: Constraining bacterial production,
498 conversion efficiency and respiration in the Ross Sea, Antarctica, January–February, 1997, *Deep Sea Research Part II: Topical Studies in*
499 *Oceanography*, 47, 3227-3247, 2000.
- 500 Ducklow, H. W., and Doney, S. C.: What is the metabolic state of the oligotrophic ocean? A debate, *Ann Rev Mar Sci*, 5, 525-533,
501 10.1146/annurev-marine-121211-172331, 2013.
- 502 Engelbrecht, J. P., Stenchikov, G., Prakash, P. J., Lersch, T., Anisimov, A., and Shevchenko, I.: Physical and chemical properties of deposited
503 airborne particulates over the Arabian Red Sea coastal plain, *Atmospheric Chemistry and Physics*, 17, 11467-11490, 2017.
- 504 Galmes, J., Kapralov, M., Copolovici, L., Hermida-Carrera, C., and Niinemets, Ü.: Temperature responses of the Rubisco maximum
505 carboxylase activity across domains of life: phylogenetic signals, trade-offs, and importance for carbon gain, *Photosynthesis research*, 123,
506 183-201, 2015.

507 Galmés, J., Hermida-Carrera, C., Laanisto, L., and Niinemets, Ü.: A compendium of temperature responses of Rubisco kinetic traits:
508 variability among and within photosynthetic groups and impacts on photosynthesis modeling, *Journal of experimental botany*, 67, 5067-
509 5091, 2016.

510 García-Corral, L., Barber, E., Gioux, A. R. d., Sal, S., Holding, J., Agustí, S., Navarro, N., Serret, P., Mozeti, P., and Duarte, C.: Temperature
511 dependence of planktonic metabolism in the subtropical North Atlantic Ocean, *Biogeosciences*, 11, 4529-4540, 2014.

512 García-Corral, L. S., Holding, J. M., Carrillo-de-Albornoz, P., Steckbauer, A., Pérez-Lorenzo, M., Navarro, N., Serret, P., Gasol, J. M.,
513 Morán, X. A. G., Estrada, M., Fraile-Nuez, E., Benítez-Barrios, V., Agustí, S., and Duarte, C. M.: Temperature dependence of plankton
514 community metabolism in the subtropical and tropical oceans, *Global Biogeochemical Cycles*, 31, 1141-1154, 10.1002/2017gb005629,
515 2017.

516 García-Martín, E. E., Daniels, C. J., Davidson, K., Davis, C. E., Mahaffey, C., Mayers, K. M. J., McNeill, S., Poulton, A. J., Purdie, D. A.,
517 Tarran, G. A., and Robinson, C.: Seasonal changes in plankton respiration and bacterial metabolism in a temperate shelf sea, *Progress in
518 Oceanography*, 10.1016/j.pocean.2017.12.002, 2017.

519 Garcías-Bonet, N., and Duarte, C. M.: Methane Production by Seagrass Ecosystems in the Red Sea, *Frontiers in Marine Science*, 4,
520 10.3389/fmars.2017.00340, 2017.

521 Gillooly, J. F., Brown, J. H., West, G. B., Savage, V. M., and Charnov, E. L.: Effects of size and temperature on metabolic rate, *science*,
522 293, 2248-2251, 2001.

523 Gillooly, J. F., Allen, A. P., West, G. B., and Brown, J. H.: The rate of DNA evolution: effects of body size and temperature on the molecular
524 clock, *Proceedings of the National Academy of Sciences of the United States of America*, 102, 140-145, 2005.

525 Hansen, H. P., and Koroleff, F.: Determination of nutrients, in: *Methods of seawater analysis*, edited by: K. Grasshoff, K. Kremling, and
526 Ehrhardt, M., Wiley-VCH Verlag, Weinheim, Germany, 159-228, 1999.

527 Harris, L. A., Duarte, C. M., and Nixon, S. W.: Allometric laws and prediction in estuarine and coastal ecology, *Estuaries and Coasts*, 29,
528 340-344, 2006.

529 Jurado, E., Dachs, J., Duarte, C. M., and Simo, R.: Atmospheric deposition of organic and black carbon to the global oceans, *Atmospheric
530 Environment*, 42, 7931-7939, 2008.

531 Kheirredine, M., Ouhssain, M., Claustre, H., Uitz, J., Gentili, B., and Jones, B.: Assessing pigment-based phytoplankton community
532 distributions in the Red Sea, *Frontiers in Marine Science*, 2017.

533 Kottuparambil, S., and Agustí, S.: PAHs sensitivity of picophytoplankton populations in the Red Sea, *Environmental Pollution*, 239, 607-
534 616, 2018.

535 Kürten, B., Al-Aidaros, A. M., Kürten, S., El-Sherbiny, M. M., Devassy, R. P., Struck, U., Zarokanellos, N., Jones, B. H., Hansen, T.,
536 Bruss, G., and Sommer, U.: Carbon and nitrogen stable isotope ratios of pelagic zooplankton elucidate ecohydrographic features in the
537 oligotrophic Red Sea, *Progress in Oceanography*, 140, 69-90, 10.1016/j.pocean.2015.11.003, 2016.

538 Levanon-Spanier, I., Padan, E., and Reiss, Z.: Primary production in a desert-enclosed sea—the Gulf of Elat (Aqaba), Red Sea, *Deep Sea
539 Research Part A: Oceanographic Research Papers*, 26, 673-685, 1979.

540 [López-Sandoval, D. C., Delgado-Huertas, A., Carrillo-de-Albornoz, P., Duarte, C. M., and Agustí, S.: Use of cavity ring-down spectrometry
541 to quantify 13C-primary productivity in oligotrophic waters, *Limnology and Oceanography: Methods*, doi:10.1002/lom3.10305,
542 doi:10.1002/lom3.10305, 2019.](#)

543 López-Urrutia, A., San Martín, E., Harris, R. P., and Irigoien, X.: Scaling the metabolic balance of the oceans, *Proceedings of the National
544 Academy of Sciences*, 103, 8739-8744, 2006.

545 Maraño, E., Cermeño, P., Huete-Ortega, M., López-Sandoval, D. C., Mouriño-Carballido, B., and Rodríguez-Ramos, T.: Resource supply
546 overrides temperature as a controlling factor of marine phytoplankton growth, *PLoS one*, 9, e99312, 2014.

547 Maraño, E., Lorenzo, M. P., Cermeño, P., and Mouriño-Carballido, B.: Nutrient limitation suppresses the temperature dependence of
548 phytoplankton metabolic rates, *The ISME journal*, 2018.

549 Osman, E. O., Smith, D. J., Ziegler, M., Kürten, B., Conrad, C., El-Haddad, K. M., Voolstra, C. R., and Suggett, D. J.: Thermal refugia
550 against coral bleaching throughout the northern Red Sea, *Global change biology*, 24, e474-e484, 2018.

551 Oudot, C., Gerard, R., Morin, P., and Gningue, I.: Precise shipboard determination of dissolved oxygen (Winkler procedure) for productivity
552 studies with a commercial system 1, *Limnology and Oceanography*, 33, 146-150, 1988.

553 Padfield, D., Lowe, C., Buckling, A., Ffrench-Constant, R., Student Research, T., Jennings, S., Shelley, F., Olafsson, J. S., and Yvon-
554 Durocher, G.: Metabolic compensation constrains the temperature dependence of gross primary production, *Ecol Lett*, 20, 1250-1260,
555 10.1111/ele.12820, 2017.

556 Pearman, J. K., Kürten, S., Sama, Y., Jones, B., and Carvalho, S.: Biodiversity patterns of plankton assemblages at the extremes of the Red
557 Sea, *FEMS microbiology ecology*, 92, fiw002, 2016.

558 Qurban, M. A., Balala, A. C., Kumar, S., Bhavya, P. S., and Wafar, M.: Primary production in the northern Red Sea, *Journal of Marine
559 Systems*, 132, 75-82, 10.1016/j.jmarsys.2014.01.006, 2014.

560 Qurban, M. A., Wafar, M., Jyothibabu, R., and Manikandan, K. P.: Patterns of primary production in the Red Sea, *Journal of Marine Systems*,
561 169, 87-98, 10.1016/j.jmarsys.2016.12.008, 2017.

562 Rahav, E., Herut, B., Mulholland, M. R., Belkin, N., Elifantz, H., and Berman-Frank, I.: Heterotrophic and autotrophic contribution to
563 dinitrogen fixation in the Gulf of Aqaba, *Marine Ecology Progress Series*, 522, 67-77, 2015.

564 Raitso, D. E., Hoteit, I., Prihartato, P. K., Chronis, T., Triantafyllou, G., and Abualnaja, Y.: Abrupt warming of the Red Sea, *Geophysical*
565 *Research Letters*, 38, n/a-n/a, 10.1029/2011gl047984, 2011.

566 Raitso, D. E., Pradhan, Y., Brewin, R. J., Stenchikov, G., and Hoteit, I.: Remote sensing the phytoplankton seasonal succession of the Red
567 Sea, *PLoS One*, 8, e64909, 10.1371/journal.pone.0064909, 2013.

568 Raitso, D. E., Yi, X., Platt, T., Racault, M.-F., Brewin, R. J. W., Pradhan, Y., Papadopoulos, V. P., Sathyendranath, S., and Hoteit, I.:
569 Monsoon oscillations regulate fertility of the Red Sea, *Geophysical Research Letters*, 42, 855-862, 10.1002/2014gl062882, 2015.

570 Rasul, N. M., and Stewart, I. C.: *The Red Sea: the formation, morphology, oceanography and environment of a young ocean basin*, Springer,
571 2015.

572 Rasul, N. M., Stewart, I. C., and Nawab, Z. A.: Introduction to the Red Sea: its origin, structure and environment., in: *The Red Sea*, edited
573 by: Rasul, N. M., and Stewart, I. C., Springer, Berlin, 1-28, 2015.

574 Regaudie-de-Gioux, A., and Duarte, C. M.: Temperature dependence of planktonic metabolism in the ocean, *Global Biogeochemical Cycles*,
575 26, 2012.

576 Regaudie-de-Gioux, A., and Duarte, C. M.: Global patterns in oceanic planktonic metabolism, *Limnology and Oceanography*, 58, 977-986,
577 doi:10.4319/lo.2013.58.3.0977, 2013.

578 Robinson, C., and Williams, P. J. I. B.: Plankton net community production and dark respiration in the Arabian Sea during September 1994,
579 *Deep Sea Research Part II: Topical Studies in Oceanography*, 46, 745-765, 1999.

580 Robinson, C., Serret, P., Tilstone, G., Teira, E., Zubkov, M. V., Rees, A. P., and Woodward, E. M. S.: Plankton respiration in the eastern
581 Atlantic Ocean, *Deep Sea Research Part I: Oceanographic Research Papers*, 49, 787-813, 2002.

582 Robinson, C., and Williams, P. J. I. B.: Respiration and its measurement in surface marine waters, *Respiration in aquatic ecosystems*, 147-180,
583 2005.

584 Robitzsch, V. S., Lozano-Cortes, D., Kandler, N. M., Salas, E., and Berumen, M. L.: Productivity and sea surface temperature are correlated
585 with the pelagic larval duration of damselfishes in the Red Sea, *Mar Pollut Bull*, 105, 566-574, 10.1016/j.marpolbul.2015.11.045, 2016.

586 Serret, P., Robinson, C., Fernández, E., Teira, E., and Tilstone, G.: Latitudinal variation of the balance between plankton photosynthesis and
587 respiration in the eastern Atlantic Ocean, *Limnology and Oceanography*, 46, 1642-1652, 2001.

588 Serret, P., Robinson, C., Fernández, E., Teira, E., Tilstone, G., and Pérez, V.: Predicting plankton net community production in the Atlantic
589 Ocean, *Deep Sea Research Part II: Topical Studies in Oceanography*, 56, 941-953, 2009.

590 Smith, S., and Mackenzie, F.: The ocean as a net heterotrophic system: implications from the carbon biogeochemical cycle, *Global*
591 *Biogeochemical Cycles*, 1, 187-198, 1987.

592 Smith, S., and Hollibaugh, J.: Coastal metabolism and the oceanic organic carbon balance, *Reviews of Geophysics*, 31, 75-89, 1993.

593 Sofianos, S., and Johns, W. E.: Water mass formation, overturning circulation, and the exchange of the Red Sea with the adjacent basins, in:
594 *The Red Sea*, Springer, 343-353, 2015.

595 Sofianos, S. S.: An Oceanic General Circulation Model (OGCM) investigation of the Red Sea circulation, 1. Exchange between the Red Sea
596 and the Indian Ocean, *Journal of Geophysical Research*, 107, 10.1029/2001jc001184, 2002.

597 Sofianos, S. S., and Johns, W. E.: Observations of the summer Red Sea circulation, *Journal of Geophysical Research*, 112,
598 10.1029/2006jc003886, 2007.

599 Thomas, M. K., Kremer, C. T., and Litchman, E.: Environment and evolutionary history determine the global biogeography of phytoplankton
600 temperature traits, *Global Ecology and Biogeography*, 25, 75-86, 10.1111/geb.12387, 2016.

601 Tilstra, A., van Hoytema, N., Cardini, U., Bednarz, V. N., Rix, L., Naumann, M. S., Al-Horani, F. A., and Wild, C.: Effects of water column
602 mixing and stratification on planktonic primary production and dinitrogen fixation on a northern Red Sea coral reef, *Frontiers in*
603 *microbiology*, 9, 2018.

604 Torfstein, A., and Kienast, S.: No Correlation Between Atmospheric Dust and Surface Ocean Chlorophyll-a in the Oligotrophic Gulf of
605 Aqaba, *Northern Red Sea*, *Journal of Geophysical Research: Biogeosciences*, 123, 391-405, 2018.

606 Wafar, M., Qurban, M. A., Ashraf, M., Manikandan, K., Flandez, A. V., and Balala, A. C.: Patterns of distribution of inorganic nutrients in
607 Red Sea and their implications to primary production, *Journal of Marine Systems*, 156, 86-98, 2016.

608 Williams, P., Raine, R. C. T., and Bryan, J. R.: Agreement between the c-14 and oxygen methods of measuring phytoplankton production-
609 reassessment of the photosynthetic quotient, *Oceanologica Acta*, 2, 411-416, 1979.

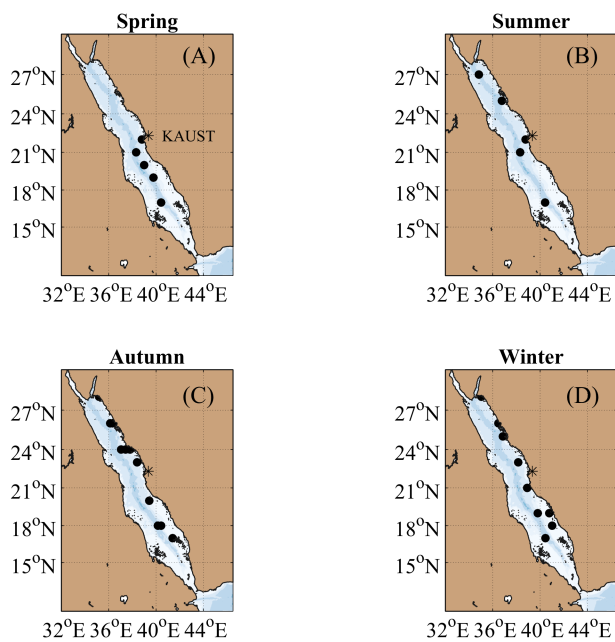
610 Williams, P.: On the definition of plankton production terms, *ICES marine science symposia*. 1993., 1993,

611 Williams, P. I. B.: The balance of plankton respiration and photosynthesis in the open oceans, *Nature*, 394, 55-57, 1998.

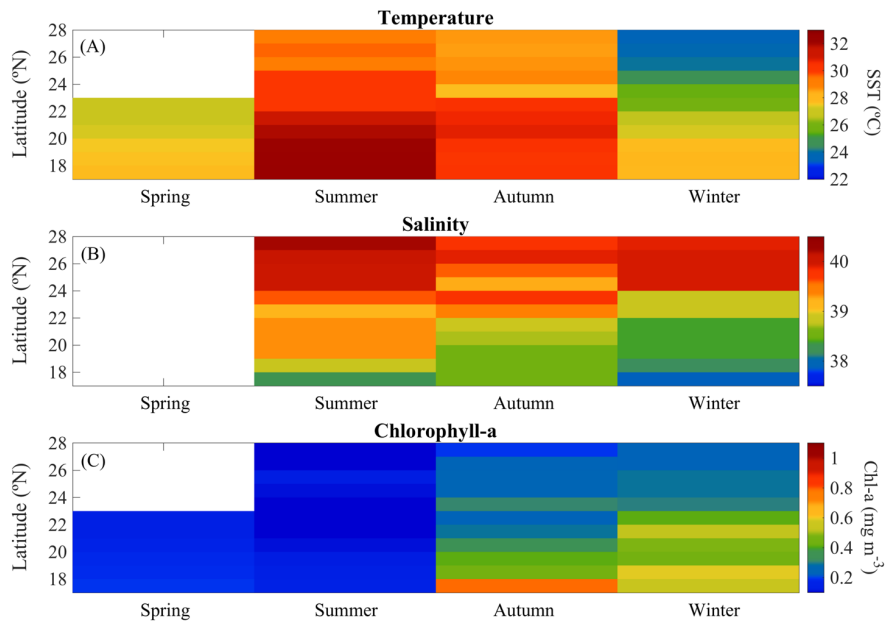
612 Williams, P. I. B., and del Giorgio, P. A.: Respiration in aquatic ecosystems: history and background, *Respiration in aquatic ecosystems*, 1-
613 17, 2005.

614 Zarokanellos, N., Papadopoulos, V. P., Sofianos, S., and Jones, B.: Physical and biological characteristics of the winter-summer transition
615 in the Central Red Sea, *Journal of Geophysical Research: Oceans*, 122, 6355-6370, <http://dx.doi.org/10.1002/2017jc012882>, 2017.

616

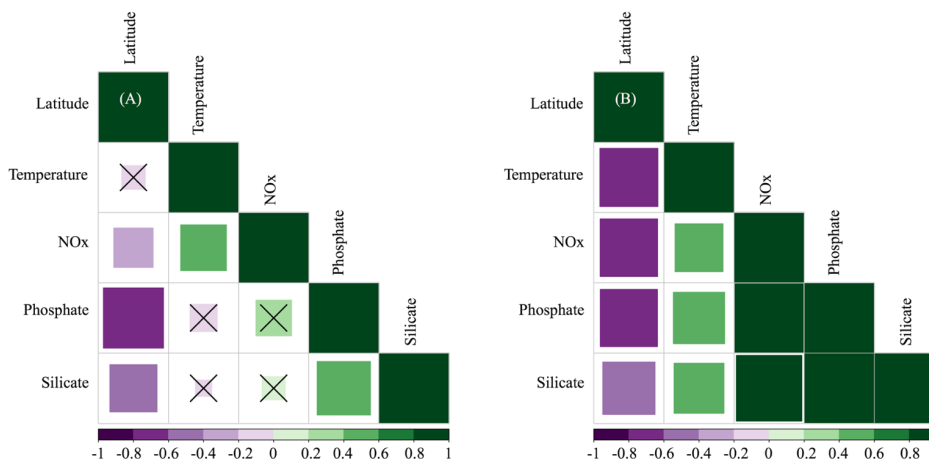


620 Figure 1: Stations sampled along the Red Sea during (A) spring (2018), (B) summer 2018, (C) autumn (2016) and (D) winter 2016 and 2017

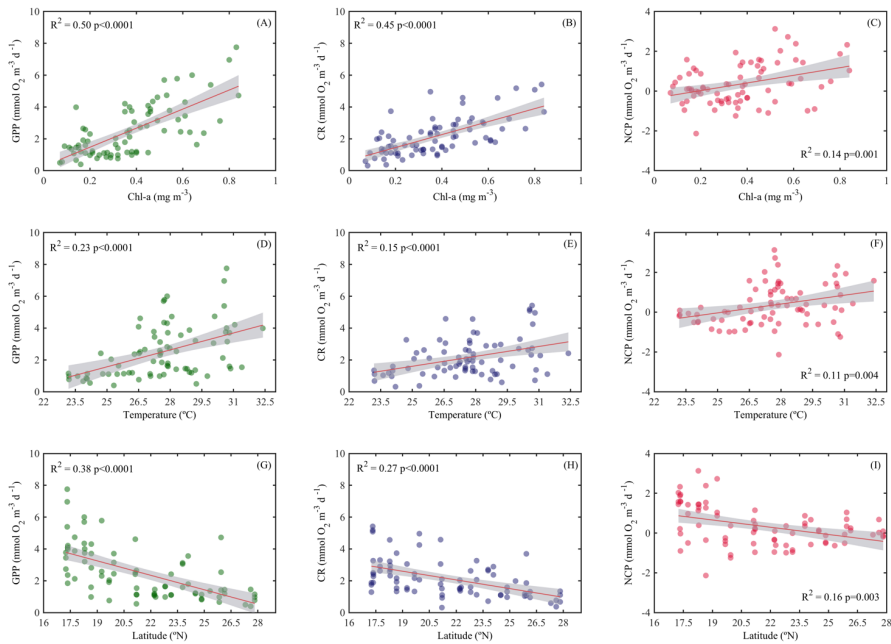


625 Figure 2: Overall seasonal and latitudinal variability of surface (A) temperature (SST), (B) salinity (C)
 and chlorophyll-a concentration (Chl-a) measured during spring (2018), summer (2017), autumn (2016)
 and winter (2016 and 2017) cruises along the Red Sea (~ 100 % of incident Photosynthetically Active
 Radiation, PAR).

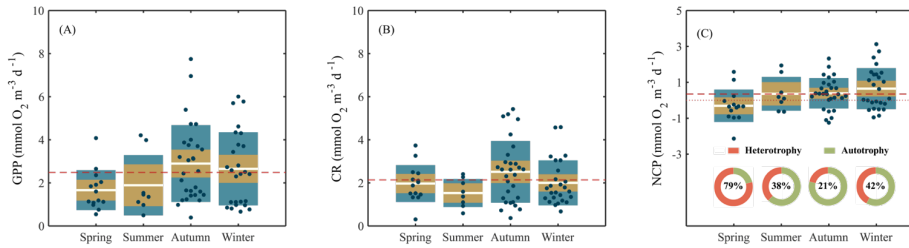
630



635 Figure 3: Pearson correlations between environmental variables (temperature and the concentrations of
 640 nitrate+nitrite [NOx], phosphate and silicate) and their latitudinal distribution measured at selected
 depths: (A) the first optical depth (from the surface down to 37% of incident PAR) and (B) at the
 bottom of the photic layer (between 1–0.1 % of incident PAR values). The size of the squares is the
 magnitude, the color indicates the direction (green for positive correlations, purple for negative
 correlations). The value of the correlation coefficient (r) is shown in the color bar below the graphs.
 Non-significant correlations are denoted with a \times .



645 Figure 4: Ordinary least squares linear regression between gross primary production (GPP), planktonic community respiration (CR) and net community production rates (NCP) with (A, B, C) Chlorophyll-a concentration (Chl-a), (D, E, F) temperature and (G, H, I) latitude. The solid red line is the linear least square fit, while the shaded grey area represents the 95% confidence intervals. The coefficient of determination and the statistical significance are indicated for each regression.



650 Figure 5. **Seasonal** variability of (A) gross primary production (GPP), (B) community respiration (CR), and (C) net community production (NCP) measured along the Red Sea. **Boxplots indicate the 95% confidence intervals** (in lighter colour), and ± 1 SD (dark shaded). The central horizontal white lines in the box mark the mean value for each season. The red dashed lines represent the overall mean while the red dotted line in (C) defines the limit between autotrophic from heterotrophic communities (NCP=0). Values inside the donut plots (C) indicate the percentage of heterotrophy (NCP<) for each season.

Deleted: Box plots illustrating the seasonal

Deleted: On each box are

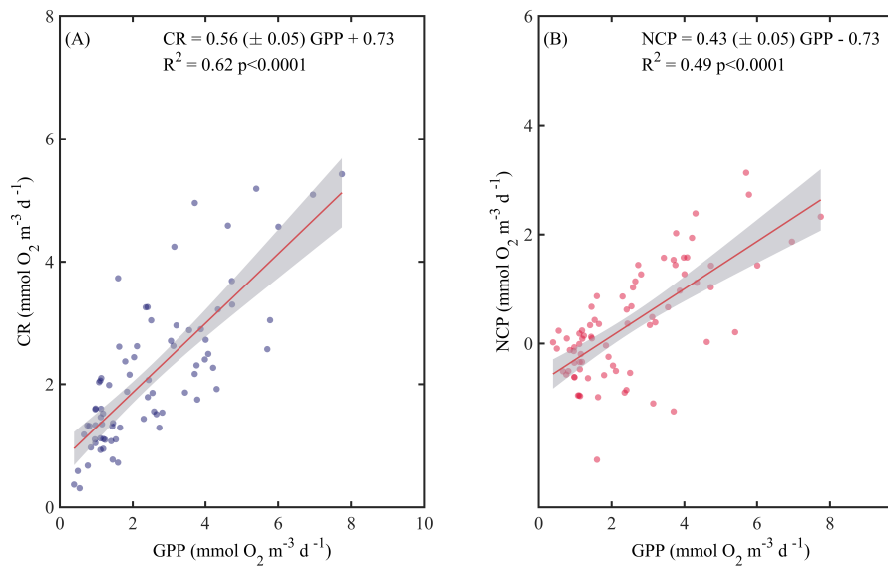
Deleted: data layed over a

Deleted: interval (shaded

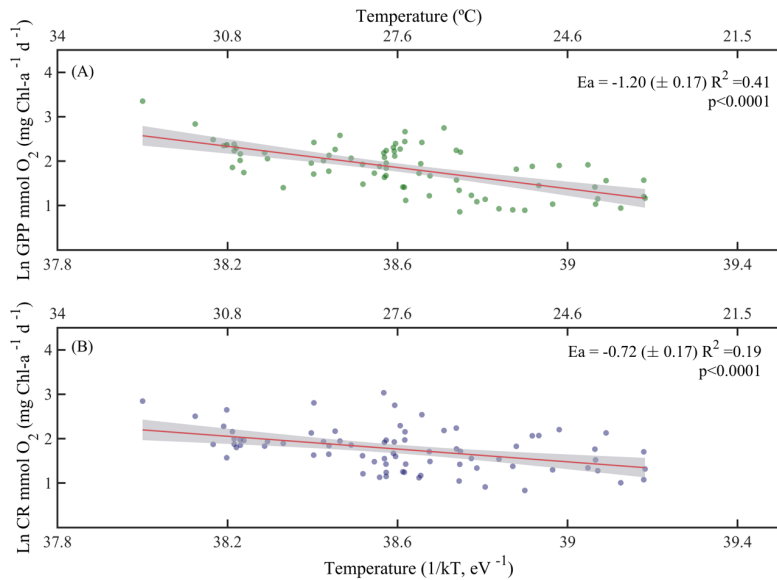
Deleted: color

Deleted: in grey

655



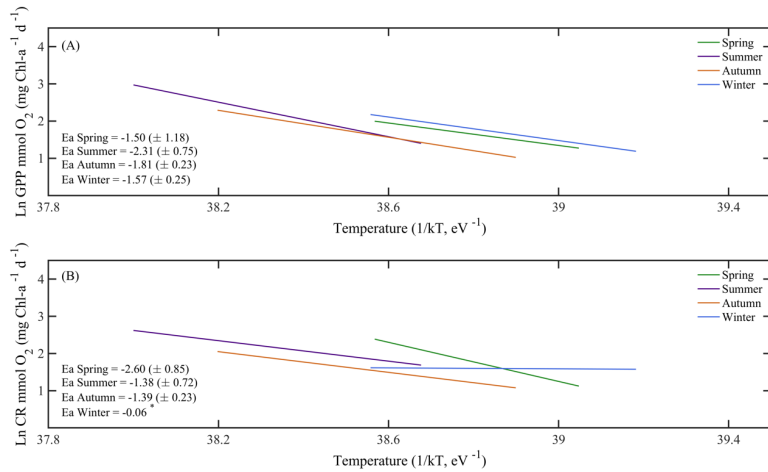
665 Figure 6: Ordinary least square linear regression between (A) planktonic community respiration and (B) net community production (NCP) with gross primary production (GPP) rates measured along the Red Sea. The ordinary least square regression parameters (slope and intercept) and the statistical significance of each regression are indicated. The solid red line represents the linear least square fit, the shaded grey area represents the 95% confidence interval.



670 Figure 7: Arrhenius plots indicating temperature dependence of planktonic metabolic rates plotted as the
 relationship between the natural logarithm of (A) chlorophyll-a normalised gross primary production,
 and (B) chlorophyll-a normalised planktonic community respiration with temperature as a function of
 1/kT (lower axis), where k is the Boltzmann's constant ($8.2 \times 10^{-5} \text{ eV K}^{-1}$), and T denotes the absolute
 675 temperature (K). The corresponding temperatures in degree Celsius are shown in the upper axis for each
 graph. The solid red line is the linear least square fit, the shaded grey area represents the 95%
 confidence interval. E_a represents the activation energy, ($E_a = -\text{slope}$).

Deleted: E_a is the slope of each plot and

Deleted: .



680

Figure 8: Arrhenius plots indicating the seasonal temperature dependence of planktonic metabolic rates plotted as the relationship between the natural logarithm of (A) chlorophyll-*a* normalised gross primary production, and (B) planktonic community respiration with temperature as a function of 1/kT (lower axis), where *k* is the Boltzmann's constant ($8.2 \times 10^{-5} \text{ eV K}^{-1}$), and *T* denotes the absolute temperature (K). Each line represents the linear least square fit. E_a represents the activation energy (E_a = -slope).

685

Deleted: E_a is the slope of each regression line and

690

695

700

705 Table 1. Pearson correlation matrix between volumetric gross primary production (GPP), planktonic community respiration (CR) and net community production (NCP) with environmental variables (temperature; latitude; nitrite+nitrate, NO_x; and Chlorophyll-a concentration, Chl-*a*). Bold numbers indicate significant relationships and the significance level is indicated with *: p<0.05*, p<0.01** and p<0.001***.

	Temperature	Latitude	NO _x	Chl- <i>a</i>	GPP	CR	NCP
GPP	0.5***	-0.6***	0.0	0.7***		0.8***	0.7***
CR	0.4***	-0.5***	<u>0.2</u>	0.7***	0.8***		0.1
NCP	0.3**	-0.4***	-0.1	0.4***	0.7***	0.1	
Chl- <i>a</i>	0.1	-0.4***	0.3*		0.7***	0.7***	0.4**

Deleted: 1

710